DALTON
FULL PAPER

Novel ruthenium(III) dimers $Na_2[\{trans\text{-}RuCl_4(Me_2SO\text{-}S)\}_2(\mu\text{-}L)]$ and $[\{mer,cis\text{-}RuCl_3(Me_2SO\text{-}S)(Me_2SO\text{-}O)\}_2(\mu\text{-}L)]$ (L = bridging heterocyclic N-donor ligand) closely related to the antimetastatic complex $Na[trans\text{-}RuCl_4(Me_2SO\text{-}S)(Him)]$ †

Elisabetta Iengo, Giovanni Mestroni, Silvano Geremia, Mario Calligaris and Enzo Alessio *

Dipartimento di Scienze Chimiche, Università di Trieste, Via L. Giorgieri 1, 34127 Trieste, Italy

Received 27th May 1999, Accepted 16th August 1999

The symmetrical dianionic and neutral ruthenium(III) dimers $Na_2[\{trans\text{-}RuCl_4(Me_2SO\text{-}S)\}_2(\mu\text{-}L)]$ **1** and $[\{mer,cis\text{-}RuCl_3(Me_2SO\text{-}S)(Me_2SO\text{-}O)\}_2(\mu\text{-}L)]$ **3** (L = pyrazine **1a**, **3a**; pyrimidine **1b**; 4,4′-bipyridine **1c**; 1,2-bis(4-pyridyl)-ethane **1d**; or 1,3-bis(4-pyridyl)propane **1e**), which represent unprecedented examples in the general Creutz–Taube family of ruthenium dimers, were developed with the specific aim of assessing their antineoplastic properties. Each ruthenium center in **1** and **3** has a co-ordination environment similar to that of known anionic and neutral monomeric ruthenium(III) complexes endowed with a specific antimetastatic activity against animal model tumors. Beside the synthesis and spectroscopic characterization of the new dimers, and the structural characterization of **1a**, **1b**, **1c**, and **3a**, a thorough investigation of their chemical behavior in aqueous solution was made. At 25 °C and pH 7.4 the dianionic species **1a**–**1e** maintain their dimeric structure and undergo rather slow stepwise chloride hydrolysis to yield the relatively inert diaqua species $[\{mer,cis\text{-}RuCl_3(Me_2SO\text{-}S)(H_2O)\}_2(\mu\text{-}L)]$. At physiological pH dimers **1a**–**1e** are also easily and quantitatively reduced by equivalent amounts of ascorbic acid to the corresponding $Ru^{II/II}$ dimers which, in turn, undergo stepwise aquation with rates roughly comparable to those of the $Ru^{III/III}$ species of equal net charge. Since the reduction processes might occur also *in vivo*, the chemical behavior of the $Ru^{II/II}$ dimers is relevant to understanding the biological mechanism of action of these compounds and was thus investigated in detail. The neutral dimer **3**, which is scarcely soluble in aqueous solution, gives soluble dimeric species upon reduction with ascorbic acid. We found that reduction is accompanied by *O* to *S* linkage isomerization and by partial dissociation of the equatorial dmso. Overall, the dimeric structures of the new compounds are quite robust, both in the $Ru^{III/III}$ and in the $Ru^{II/II}$ form, and they undergo aquation reactions similar to those of the monomeric analogs. However, while the monomeric species after aquation are either mono- or bi-functional binders, the new dimers might behave as bi- or even tetra-functional binders. Thus, it is likely that their interaction with biological targets might lead to adducts which are not accessible to the mononuclear species.

Introduction

In recent years we have described the selective antimetastatic properties of an anionic ruthenium(III) compound, $Na[trans\text{-}RuCl_4(Me_2SO\text{-}S)(Him)]$ **NAMI** (Him = imidazole), against several animal tumor models.[1] More recently, the corresponding imidazolium salt, $[H_2im][trans\text{-}RuCl_4(Me_2SO\text{-}S)(Him)]$ **NAMI-A**, was synthesized by us with the aim of improving the solid state stability of the complex.[2] Overall, the biological and chemical characteristics of **NAMI-A** were such to warrant its clinical development and the complex is currently entering phase I clinical trials as an antimetastatic drug.[3]

The experience accumulated in these years in the field of ruthenium antitumor compounds allowed us to formulate a rough structure–activity relationship: anionic or neutral ruthenium(III) chloride complexes bearing at least one N-donor ligand (L) in their co-ordination sphere are likely to possess some activity. In fact, several compounds of general formula $Na[trans\text{-}RuCl_4(Me_2SO\text{-}S)(L)]$, $mer,cis\text{-}[RuCl_3(Me_2SO)_2(L)]$ and $[HL][trans\text{-}RuCl_4(L)_2]$, developed by us[4] and by the group of Keppler,[5] were found to be active against animal tumors. Interestingly, $[H_2im][trans\text{-}RuCl_4(Him)_2]$ **ICR** and $[H_2ind][trans\text{-}RuCl_4(Hind)_2]$ (Hind = indazole) are active against platinum-resistant colorectal tumors.[6] With the exception of ammonia in $Na[trans\text{-}RuCl_4(Me_2SO\text{-}S)(NH_3)]$ and $mer,cis\text{-}[RuCl_3(Me_2SO)_2(NH_3)]$, for all the other compounds heterocyclic N-donor ligands were used. Moreover, the ruthenium(III) compounds which bear a Me_2SO-*S* molecule in their co-ordination sphere have an additional distinctive feature: by virtue of the π-acceptor properties of S-bonded dmso the reduction potential of such species is remarkably high (**NAMI-A**, 253 *vs.* **ICR**, −240 mV),[4] thus making *in vivo* reduction to ruthenium(II) active species a very likely process.

We wanted now to explore new structural features and reasoned that treatment of the well known ruthenium(III) dmso precursors, $Na[trans\text{-}RuCl_4(Me_2SO\text{-}S)_2]$ and $mer\text{-}[RuCl_3(Me_2SO)_3]$, with ditopic non-chelating N-ligands, instead of monodentate ligands, might lead to new dimeric species in which each ruthenium center would nevertheless maintain a co-ordination environment very similar to that in the active monomeric compounds. The platinum dimers and trimers developed by Farrell,[7] one of which is currently in phase I clinical trials, represent a very stimulating precedent in this sense. Dimers such as $[\{PtCl_2(NH_3)\}_2(NH_2(CH_2)_nNH_2)]$, ideally derived from $cis\text{-}[PtCl_2(NH_3)_2]$ upon replacement of one ammonia with a bridging aliphatic diamine, maintain structural motifs and co-ordination environments very similar to those of the monomeric parent compound (cisplatin); they are as active as cisplatin against conventional tumor lines but are remarkably active also against tumor lines resistant to cisplatin, apparently because the co-ordination-induced modifications of DNA are different from those induced by the mononuclear complex. It is therefore reasonable that also in the case of ruthenium, even

† *Supplementary data available*: rotatable 3-D crystal structure diagram in CHIME format. See http://www.rsc.org/suppdata/dt/1999/3361/

though there is yet no proof that the mechanism of action is related to DNA co-ordination, dimeric species might maintain the antineoplastic activity of the closely related mononuclear species but with some different, and possibly enhanced, selectivity or specificity.

We report here the synthesis and characterization of new dianionic and neutral symmetrical ruthenium(III) dimers of formula $Na_2[\{trans\text{-}RuCl_4(Me_2SO\text{-}S)\}_2(\mu\text{-}L)]$ and $[\{mer,cis\text{-}RuCl_3(Me_2SO\text{-}S)(Me_2SO\text{-}O)\}_2(\mu\text{-}L)]$, respectively, in which L is a bridging heterocyclic N-ligand such as pyrazine (pyz).[8]

In the chemistry of ruthenium there are many examples of robust cationic dimers in which the two units are held together by a pyrazine-like bridging ligand.[9] These dimers are mainly based either on the $Ru(NH_3)_5^{2+/3+}$ fragments, and thus belong to the well known Creutz–Taube ion family $[\{Ru(NH_3)_5\}_2(\mu\text{-}L)]^{n+}$ ($n = 4$, 5, or 6),[10] or on polypyridyl $Ru^{2+/3+}$ fragments.[11] While the synthetic effort has been concentrated on the production of cationic dimers, not many examples of anionic ruthenium dimers can be found in the literature. In fact, although anionic iron–cyano and osmium–cyano dimers, such as $[\{Fe(CN)_5\}_2(\mu\text{-pyz})]^{n-}$ and $[\{Os(CN)_5\}_2(\mu\text{-pyz})]^{n-}$ ($n = 4$, 5, or 6), have been described,[12,13] we are aware only of the recently reported ruthenium(II) compound $[\{Ru(hedta)\}_2(\mu\text{-pyz})]^{2-}$ (H_3hedta = *N*-carboxymethyl-*N*′-(hydroxyethyl)ethylenediiminotriacetic acid).[14]

Results and discussion

Synthesis of the complexes

The bridging ligands. The following, commercially available, bridging N-ligands (L) were used (Chart 1): pyrazine (pyz), pyrimidine (pym), 4,4′-bipyridine (bipy), 1,2-bis(4-pyridyl)-ethane (etbipy), and 1,3-bis(4-pyridyl)propane (prbipy). This relatively small series of ligands nevertheless allowed us to vary parameters such as the relative disposition of the two ruthenium(III) centers (*e.g.* 180° with pyz *vs.* 120° with pym), their distance (*e.g.* pyz *vs.* bipy), and the electronic conjugation and flexibility of the linker. Although the reactions with pyrazine will be described in more detail, similar results were obtained also with the other bridging ligands unless otherwise stated.

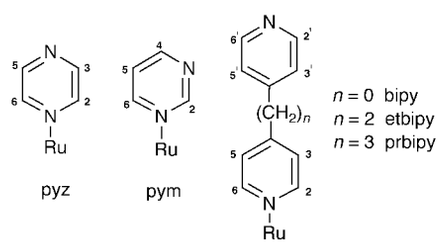

Chart 1 Schematic structures of the ditopic L ligands with numbering schemes when co-ordinated to ruthenium.

Dianionic dimers $Na_2[\{trans\text{-}RuCl_4(Me_2SO\text{-}S)\}_2(\mu\text{-}L)]$ 1a–1e. We have shown that in the ruthenium(III) precursor $Na[trans\text{-}RuCl_4(Me_2SO\text{-}S)_2]$ one of the two *trans* Me_2SO-*S* ligands is easily replaced by an N-donor ligand L to yield anionic compounds of formula $Na[trans\text{-}RuCl_4(Me_2SO\text{-}S)(L)]$.[4] Similarly, we found now that treatment of $Na[trans\text{-}RuCl_4(Me_2SO\text{-}S)_2]$ with 0.5 equivalent of the ditopic pyz ligand at room temperature led, with good selectivity and yield, to the dianionic dimer $Na_2[\{trans\text{-}RuCl_4(Me_2SO\text{-}S)\}_2(\mu\text{-pyz})]$ **1a**. Conversely, when an excess of pyz was used, the monomeric species $Na[trans\text{-}RuCl_4(Me_2SO\text{-}S)(pyz)]$ **2a**, in which only one basic site of pyz is bound to Ru^{III}, was obtained (Scheme 1). Beside elemental analysis, **1a** and **2a** have also some distinctive spectroscopic features which are characteristic, respectively, of their dimeric or monomeric nature. Infrared spectroscopy is diagnostic of the

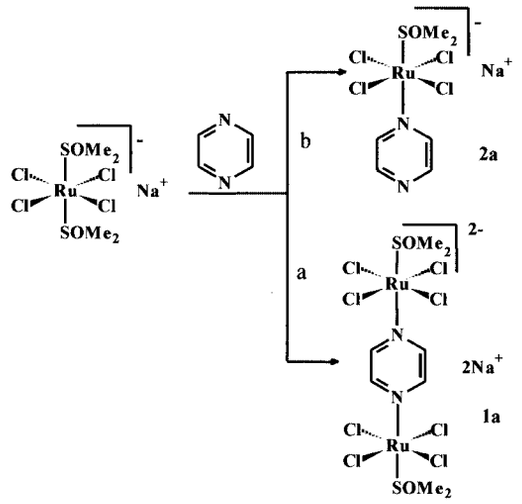

Scheme 1 Reactivity pathways of $Na[trans\text{-}RuCl_4(Me_2SO\text{-}S)_2]$ with pyrazine leading either to the dimer $Na_2[\{trans\text{-}RuCl_4(Me_2SO\text{-}S)\}_2(\mu\text{-pyz})]$ **1a** (path a, pyz:Ru = 0.5:1) or to the monomer $Na[trans\text{-}RuCl_4(Me_2SO\text{-}S)(pyz)]$ **2a** (path b, pyz:Ru = 5:1).

binding mode (terminal or bridging) of pyrazine.[15] In the solid state mono-co-ordinated pyrazine is characterized by an IR active "breathing mode" which gives a sharp band at about 1590 cm^{-1} (1590 cm^{-1} for **2a**); this absorption becomes considerably less intense and moves to higher frequencies when pyrazine is symmetrically bound to two metal centers (1650 cm^{-1} for **1a**). The ^1H NMR spectrum of **2a** (D_2O), besides the typical broad resonance for S-bonded dmso at about δ −14, shows a broad signal at about δ −2 that integrates approximately for two protons and was attributed to the pyrazine protons adjacent to the unbound N atom ($H^{3,5}$), and a very broad resonance centered at δ −7 attributed to the $H^{2,6}$ protons. In agreement with this finding in **1a** the resonance of the four equivalent pyz protons, which are all close to a paramagnetic ruthenium(III) center, is broadened beyond detection and only the Me_2SO-*S* signal at about δ −14 was detected.

In a similar manner, treatment of the anionic precursor $Na[trans\text{-}RuCl_4(Me_2SO\text{-}S)_2]$ with the appropriate amount of each ditopic L ligand led to the isolation of the corresponding dimers of general formula $Na_2[\{trans\text{-}RuCl_4(Me_2SO\text{-}S)\}_2(\mu\text{-L})]$ (L = pym **1b**, bipy **1c**, etbipy **1d**, or prbipy **1e**). The NMR spectrum of each dimer is characterized by the broad resonance for S-bonded sulfoxides at about δ −14; other broad signals deriving from the bridging ligands were assigned (see Experimental section) according to the criterion that the sharper resonances correspond to protons which are further removed from the paramagnetic ruthenium(III) centers.

Neutral dimer $[\{mer,cis\text{-}RuCl_3(Me_2SO\text{-}S)(Me_2SO\text{-}O)\}_2(\mu\text{-pyz})]$ 3a. Similarly to the anionic species, treatment of the neutral ruthenium(III) precursor $mer,trans\text{-}[RuCl_3(Me_2SO\text{-}S)_2(Me_2SO\text{-}O)]$ with pyz involved selective replacement of one of the two *trans* S-bonded sulfoxides and led either to the dimeric species $[\{mer,cis\text{-}RuCl_3(Me_2SO\text{-}S)(Me_2SO\text{-}O)\}_2(\mu\text{-pyz})]$ **3a** or to the monomeric compound $mer,cis\text{-}[RuCl_3(Me_2SO\text{-}S)(Me_2SO\text{-}O)(pyz)]$ **4a**, depending on the pyz:Ru ratio. The spectroscopic features of the sulfoxides in the monomer **4a** are similar to those found for the corresponding complexes with monodentate L ligands described by us:[4] S–O stretching bands at about 1100 (Me_2SO-*S*) and 900 cm^{-1} (Me_2SO-*O*) in the solid state IR spectrum, and broad resonances at δ −12.7 (Me_2SO-*S*) and 9.1 (Me_2SO-*O*) in the solution ^1H NMR spectrum. The presence of terminal pyrazine in **4a** is indicated by the typical IR stretching band at about 1600 cm^{-1} and by the broad NMR resonance at δ −0.6 attributed to $H^{3,5}$. Both these spectroscopic features of pyrazine are absent in the corresponding spectra of the dimeric species **3a**, in agreement with the symmetrical co-

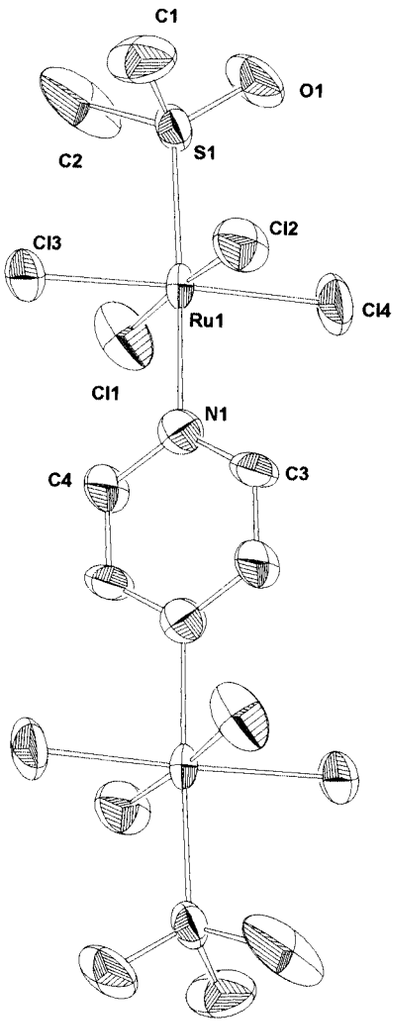

Fig. 1 An ORTEP[16] view of the anion of $Na_2[\{trans\text{-}RuCl_4(Me_2SO\text{-}S)\}_2(\mu\text{-pyz})]$ **1a** (thermal ellipsoids at 50% probability) with the atom labeling scheme.

ordination of the ligand to two ruthenium centers. The neutral dimer **3a** is soluble in dimethyl sulfoxide, but sparingly soluble in water; for this reason the synthesis was not extended to the other bridging ligands.

Crystal structures

The dimeric complexes **1** usually precipitate with three molecules of dmso and a molecule of (adventitious) water of crystallization; interestingly, in the case of **1a** and **1b** the three sulfoxide molecules are maintained also when the dimers are recrystallized from water (see Experimental section).

The dinuclear anions of $Na_2[\{trans\text{-}RuCl_4(Me_2SO\text{-}S)\}_2(\mu\text{-pyz})]$ **1a** (Fig. 1) and $Na_2[\{trans\text{-}RuCl_4(Me_2SO\text{-}S)\}_2(\mu\text{-bipy})]$ **1c** (Fig. 2), as well as the neutral complex $[\{mer,cis\text{-}RuCl_3(Me_2SO\text{-}S)(Me_2SO\text{-}O)\}_2(\mu\text{-pyz})]$ **3a** (Fig. 3), lie on crystallographic inversion centers located on the mass center of the bridging ligands. These therefore are strictly planar and the two ruthenium equatorial planes are parallel to each other. The dinuclear anion of $Na_2[\{trans\text{-}RuCl_4(Me_2SO\text{-}S)\}_2(\mu\text{-pym})]$ **1b** (Fig. 4) displays a pseudo C_{2v} symmetry coincident with that of the ligand. The ligand plane (r. m. s. deviation 0.005 Å) is roughly perpendicular to both the $RuCl_4$ planes (r. m. s. deviation 0.022 Å) with which it forms dihedral angles of 83.7 and 88.9°, respectively. These in turn are inclined at 61.6°.

The orientation of the nitrogen bases, with respect to the equatorial co-ordination planes, can be described by the torsion angle X–Ru–N–Cα, ψ (X = Cl for **1a**–**1c**, and O for **3a**), in which X and Cα are chosen so that ψ is less than 90°. Tables 1–3

Table 1 Selected bond distances (Å) and angles (°) for $Na_2[\{trans\text{-}RuCl_4(Me_2SO\text{-}S)\}_2(\mu\text{-pyz})]$ **1a** and $Na_2[\{trans\text{-}RuCl_4(Me_2SO\text{-}S)\}_2(\mu\text{-bipy})]$ **1c**

	1a·3Me_2SO·H_2O	**1c**·5.6H_2O
Ru–Cl(1)	2.327(7)	2.362(1)
Ru–Cl(2)	2.341(6)	2.382(1)
Ru–Cl(3)	2.321(5)	2.312(1)
Ru–Cl(4)	2.339(6)	2.342(2)
Ru–S	2.275(5)	2.306(1)
Ru–N(1)	2.11(2)	2.117(4)
S–O	1.45(1)	1.483(4)
S–C(1)	1.72(2)	1.754(6)
S–C(2)	1.76(2)	1.778(6)
S–Ru–N(1)	177.1(6)	177.1(1)
Ru–N(1)–C(3)	121(1)	120.4(3)
Ru–N(1)–C(4)	122(1)	122.5(3)
C(3)–N(1)–C(4)	116(2)	117.1(4)
Ru–S–O	120.3(7)	117.1(2)
Ru–S–C(1)	110.4(8)	113.5(2)
Ru–S–C(2)	112.0(9)	112.6(2)
O–S–C(1)	106(1)	105.8(3)
O–S–C(2)	104(1)	106.6(3)
C(1)–S–C(2)	102(2)	99.6(4)
Torsion angles		
Cl(4)–Ru–S–O	−1.8(9)	−23.5(2)
Cl(4)–Ru–N(1)–C(3)	47(2)	−51.0(3)

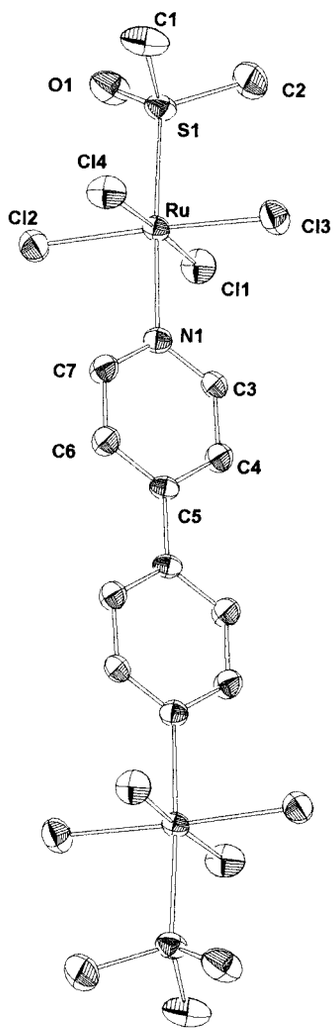

Fig. 2 An ORTEP view of the anion of $Na_2[\{trans\text{-}RuCl_4(Me_2SO\text{-}S)\}_2(\mu\text{-bipy})]$ **1c**. Details as in Fig. 1.

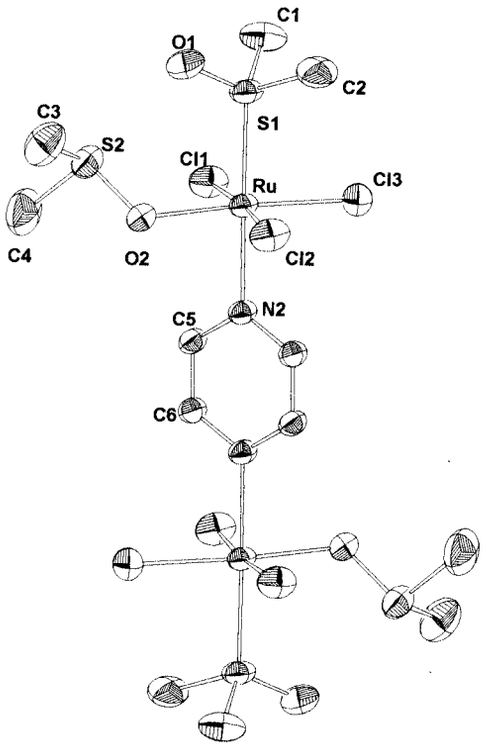

Fig. 3 An ORTEP view of [{*mer*,*cis*-$RuCl_3(Me_2SO$-*S*)(Me_2SO-*O*)}$_2$-(μ-pyz)] **3a**. Details as in Fig. 1.

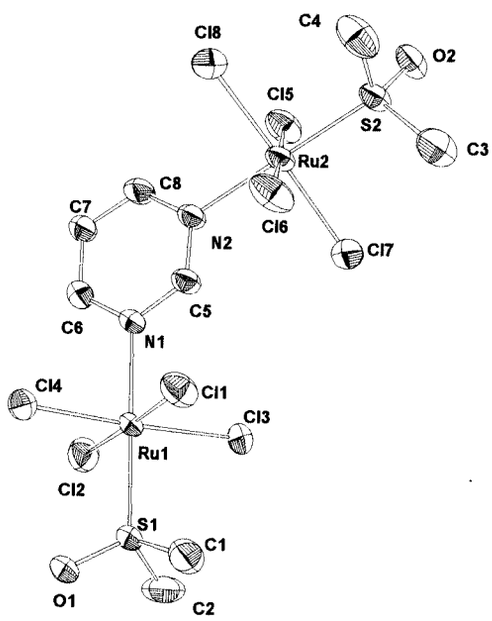

Fig. 4 An ORTEP view of the anion of Na_2[{*trans*-$RuCl_4(Me_2$-SO-*S*)}$_2$(μ-pym)] **1b**. Details as in Fig. 1.

show that ψ ranges from 45.7 to 51.0°, averaging to 48°, so that, in all these compounds, the ligand approximately bisects one Cl–Ru–Cl bond angle, as expected from intramolecular interactions. As for the orientation of the dimethyl sulfoxide ligands, it is interesting that the Me_2SO-*S* ligands are always oriented in such a way that the S–O bonds nearly eclipse the equatorial coordination bond Ru–X, as shown by the torsion angles X–Ru–S–O which range from 1.8 to 23.5°. Interestingly, the average value of 10° corresponds to the most frequent conformation observed in Ru^{III}–S complexes.[17] In **3a** the conformation of the Ru–Me_2SO-*O* moiety, described by the two Ru–O–S–C torsion angles of about ±128.5°, confirms that O-bonded sulfoxides have a general preference for the *trans*-*trans* orientation of the methyl groups.[17]

Table 2 Selected bond distances (Å) and angles (°) for Na_2[{*trans*-$RuCl_4(Me_2SO$-*S*)}$_2$(μ-pym)] **1b**

Ru(1)–Cl(1)	2.361(2)	Ru(2)–Cl(5)	2.359(1)
Ru(1)–Cl(2)	2.338(2)	Ru(2)–Cl(6)	2.322(1)
Ru(1)–Cl(3)	2.344(1)	Ru(2)–Cl(7)	2.342(2)
Ru(1)–Cl(4)	2.352(1)	Ru(2)–Cl(8)	2.364(2)
Ru(1)–S(1)	2.281(1)	Ru(2)–S(2)	2.291(1)
Ru(1)–N(1)	2.122(4)	Ru(2)–N(2)	2.127(4)
S(1)–O(1)	1.482(3)	S(2)–O(2)	1.479(3)
S(1)–C(1)	1.776(6)	S(2)–C(3)	1.777(5)
S(1)–C(2)	1.754(6)	S(2)–C(4)	1.754(7)
S(1)–Ru(1)–N(1)	177.1(1)	S(2)–Ru(2)–N(2)	177.8(1)
Ru(1)–N(1)–C(3)	121.1(3)	Ru(2)–N(2)–C(5)	120.3(3)
Ru(1)–N(1)–C(4)	120.7(3)	Ru(2)–N(2)–C(8)	122.6(3)
C(3)–N(1)–C(4)	118.2(4)	C(5)–N(2)–C(8)	117.1(4)
Ru(1)–S(1)–O(1)	118.8(2)	Ru(2)–S(2)–O(2)	118.2(2)
Ru(1)–S(1)–C(1)	112.0(2)	Ru(2)–S(2)–C(3)	112.5(2)
Ru(1)–S(1)–C(2)	111.5(2)	Ru(2)–S(2)–C(4)	111.1(2)
O(1)–S(1)–C(1)	105.7(3)	O(2)–S(2)–C(3)	105.7(3)
O(1)–S(1)–C(2)	106.6(3)	O(2)–S(2)–C(4)	107.9(3)
C(1)–S(1)–C(2)	100.5(4)	C(3)–S(2)–C(4)	99.8(4)
Torsion angles			
Cl(4)–Ru(1)–S(1)–O(1)	13.8(2)	Cl(5)–Ru(2)–S(2)–O(2)	−3.4(2)
Cl(4)–Ru(1)–N(1)–C(3)	−49.5(4)	Cl(5)–Ru(2)–N(2)–C(8)	−47.8(4)

Table 3 Selected bond distances (Å) and angles (°) for [{*mer*,*cis*-$RuCl_3(Me_2SO$-*S*)(Me_2SO-*O*)}$_2$(μ-pyz)] **3a**

Ru–Cl(1)	2.3264(9)	S(1)–O(1)	1.474(3)
Ru–Cl(2)	2.3467(9)	S(1)–C(1)	1.766(4)
Ru–Cl(3)	2.322(1)	S(1)–C(2)	1.767(4)
Ru–O(2)	2.081(2)	S(2)–O(2)	1.555(2)
Ru–N(1)	2.109(2)	S(2)–C(3)	1.782(4)
Ru–S(1)	2.2774(8)	S(2)–C(4)	1.774(4)
S(1)–Ru–N(1)	177.70(7)	O(1)–S(1)–C(1)	107.3(2)
Ru–N(1)–C(5)	121.9(2)	O(1)–S(1)–C(2)	107.0(2)
Ru–N(1)–C(6)	121.2(2)	C(1)–S(1)–C(2)	100.6(2)
C(5)–N(1)–C(6)	117.0(2)	Ru–O(2)–S(2)	121.6(1)
Ru–S(1)–O(1)	116.1(1)	O(2)–S(2)–C(3)	104.2(2)
Ru–S(1)–C(1)	113.0(1)	O(2)–S(2)–C(4)	102.3(2)
Ru–S(1)–C(2)	111.5(1)	C(3)–S(2)–C(4)	99.6(3)
Torsion angles			
O(2)–Ru–S(1)–O(1)	8.7(2)	Ru–O(2)–S(2)–C(3)	−127.8(2)
O(2)–Ru–N(1)–C(7)	45.7(2)	Ru–O(2)–S(2)–C(4)	128.9(2)

The structural parameters of the present Ru^{III}–Me_2SO compounds (Table 4) are very close to the average values previously reported for analogous complexes.[4,18] The present data confirm the observation that while the Ru^{III}–X (X = N, O, or Cl) bond distances decrease (0.02–0.06 Å) with respect to the Ru^{II}–X analogs, the Ru^{III}–S distances, *trans* to X, are slightly longer than the corresponding Ru^{II}–S distances (mean values 2.280(6) and 2.253(3) Å for Ru^{III} and Ru^{II}, respectively).[17] This shows that the π back-bonding contribution is markedly reduced in the ruthenium(III) complexes. On the other hand, the Ru^{III}–S distances, *trans* to X, are shorter than those *trans* to S (mean values, 2.280(6) *vs.* 2.343(3) Å), as expected from the mutual *trans* influence of the S-ligands.[17]

Chemical behavior in aqueous solution

Since these dimeric complexes were developed with the specific aim of assessing their antitumor activity,[8,19] we were interested in establishing their chemical behavior in aqueous solution, with particular regard to the physiological conditions and in comparison with the behavior of [H_2im][*trans*-$RuCl_4(Me_2$-SO-*S*)(Him)] **NAMI-A**.

All dimeric species **1a–1e** are well soluble in aqueous solution and their electronic spectra are characterized by an intense absorption between 390 and 400 nm (ε 6000–11000 dm^3 mol^{-1}

Table 4 Average bond distances (Å) and angles (°) with their probable error in parentheses for complexes **1a**, **1b**, **1c**, and **3a** (column 1) compared to average values found in the literature (column 2);[a] σ represents the standard deviation of the number of observations, n

			σ	n
Ru–Cl	2.342(4)	2.331(9)	0.018	19
Ru–S	2.286(6)	2.275(9)	0.013	5
Ru–N	2.117(3)	2.10(1)	0.008	5
S–O	1.474(6)	1.474(2)	0.014	5
S–C	1.763(6)	1.779(2)	0.019	10
O–S–C	106.3(3)	107.1(2)	1.1	10
C–S–C	100.5(4)	98.9(5)	0.9	5
Ru–S–O	118.1(7)	116.1(6)	1.6	5
Ru–S–C	112.0(3)	113.0(3)	0.9	10

[a] Average values from ref. 17.

cm^{-1}) associated with a less intense transition at about 460 nm (ε *ca.* 900 $dm^3\ mol^{-1}\ cm^{-1}$). This spectral pattern, attributed to a charge transfer transition from the chlorides to Ru^{III},[20] is typical of the $RuCl_4^-$ unit and is present also for the monomeric species. The time profiles of the electronic spectra were used to establish the solution chemical behavior of the dimers. As assessed from the decrease of the main absorption band with time (≤2% per hour at 25.0 °C), all dimers ([Ru] = 0.2 mmol dm^{-3}) are more inert than **NAMI-A** in aqueous solution. Under physiological conditions (0.1 mol dm^{-3} phosphate buffer, pH 7.4, 0.9% NaCl) the dianionic dimers **1a–1e** are considerably less inert than in water and they undergo spectral changes qualitatively similar to those observed for **NAMI-A** under the same conditions and attributed to stepwise chloride hydrolysis. In the first step the main absorption band is gradually replaced by a new absorption at about 360 nm; this process has an autocatalytic time profile (spectral changes that gradually increase with time) (Fig. 5). The new spectral feature is typical of a charge transfer transition from chloride to Ru^{III} in a *mer*-$RuCl_3$ unit,[20] and was thus attributed to the neutral dimeric species [{*mer*,*cis*-$RuCl_3(Me_2SO\text{-}S)(H_2O)$}$_2$(μ-L)] derived from **1** upon hydrolysis of two chlorides, one from each ruthenium unit.‡ The clean isosbestic points maintained in each case (**1a–1e**) in the first step (Fig. 5) suggest that the dimeric structures are stable and that only two species are present in solution in this phase.§ However, a monoanionic intermediate, [{*mer*,*cis*-$RuCl_3(Me_2SO\text{-}S)(H_2O)$}(μ-L){*trans*-$RuCl_4(Me_2SO\text{-}S)$}]$^-$, must form during the double hydrolytic process and it is unlikely that this species has a negligible concentration throughout the process. The spectral behavior observed might be explained assuming that the two halves of each dimer behave independently; in this way the dimers can be considered as the sum of two equal monomeric species, each bearing half a bridging ligand. Thus the global hydrolytic process may be written as in eqn. (1) and hence involves only two species.

$$2\textit{trans}\text{-}[RuCl_4(Me_2SO\text{-}S)(\tfrac{1}{2}\mu\text{-}L)]^- \longrightarrow 2\textit{mer}\text{-}[RuCl_3(Me_2SO\text{-}S)(H_2O)(\tfrac{1}{2}\mu\text{-}L)] + 2Cl^- \quad (1)$$

Remarkably, while the rates of first chloride hydrolysis for complexes **1c–1e** are roughly comparable to that of **NAMI-A** (half-life of *ca.* 30 min at 25.0 °C), the dimers **1a** and **1b** are considerably more inert than **NAMI-A** (half-life of about 120 min at 25.0 °C) (Fig. 6). For comparison, in the monomeric species Na[*trans*-$RuCl_4(Me_2SO\text{-}S)$(pyz)] **2a** the first hydrolytic step occurs with a rate which is intermediate between that for **NAMI-A** and that for the corresponding dimer **1a** (Fig. 6). Apparently, the rate of the first hydrolytic step depends on the basicity of the heterocyclic base. In fact it is slower for **2a** (pK_a pyz = 0.6)[14] compared to that for **NAMI-A** (pK_a Him = 6.95). Moreover, the further decrease observed from **2a** to **1a** might correspond to a lower basicity of bridging pyz (**1a**) compared to that of terminal pyz (**2a**). It has been established that while co-ordination of pyrazine to the ruthenium(II) center in $[Ru(NH_3)_5]^{2+}$ actually increases the basicity of the ligand, co-ordination to the corresponding ruthenium(III) fragment decreases it.[21] Reasonably, the decrease of basicity of the

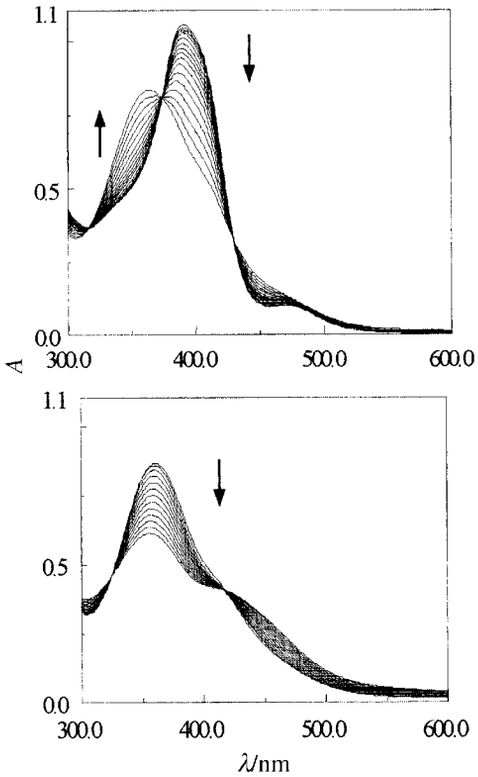

Fig. 5 Spectral changes in the visible region during stepwise chloride hydrolysis from Na_2[{*trans*-$RuCl_4(Me_2SO\text{-}S)$}$_2$(μ-pyz)] **1a** (25.0 °C, 0.1 mol dm^{-3} phosphate buffer, pH 7.4, 0.9% NaCl, [**1a**] = 10^{-4} mol dm^{-3}, scan-time interval = 10 min). Top, first step; bottom, second step.

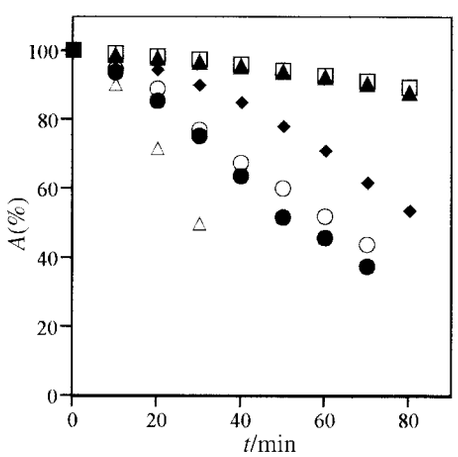

Fig. 6 Concentration time profiles of the dimers **1a**–**1e** during the first hydrolytic step (assessed by the decrease of the main absorption band in the visible spectrum) compared to that of **2a**. □ **1a**; ▲ **1b**; ● **1c**; ○ **1d**; △ **1e**; ◆ **2a**.

‡ For comparison, the absorption spectrum of complex **1a** after the first step is also very similar to that of [{*mer*,*cis*-$RuCl_3(Me_2SO\text{-}S)(Me_2SO\text{-}O)$}$_2$(μ-pyz)] **3a** in dmso solution, in which co-ordinated water is formally replaced by Me_2SO-*O*.

§ Both species derived from an hypothetical breakdown of the dimer, *i.e.* [*trans*-$RuCl_4(Me_2SO\text{-}S)(H_2O)$]$^-$ and [*trans*-$RuCl_4(Me_2SO\text{-}S)$(L)]$^-$ would undergo chloride hydrolysis, thus generating a number of species not compatible with the presence of isosbestic points. As reported by us, the aqua species [*trans*-$RuCl_4(Me_2SO\text{-}S)(H_2O)$]$^-$ is particularly labile at physiological pH (see ref. 27).

bridging ligand upon co-ordination to the first ruthenium(III) center is marked with pyz and pym, while it might become less relevant for bipy, etbipy, and prbipy in which the two basic sites are further removed from each other and less conjugated. This would explain why chloride hydrolysis for **1c**, **1d**, and **1e** is faster than for **1a** and **1b**.

The first hydrolytic step is followed by a second, slower process ($t_{\frac{1}{2}}$ of some hours at 25 °C), attributed to the hydrolysis of further chlorides. This step involves the decrease of the 360 nm band of the neutral dimers (Fig. 5); for the more labile dimers **1c**–**1e** the growth of an absorption band at higher frequencies (*ca.* 300 nm) was observed. In all cases, for observation times greater than 2 h a slow but steady increase of the absorption background was observed (the solutions turned dark green), presumably associated with the formation of polynuclear μ-oxo aggregates.

Effect of biological reducing agents

In the case of **NAMI-A** we demonstrated that, at physiological pH, addition of small amounts (with respect to Ru) of biological reductants such as cysteine and ascorbic acid remarkably enhanced the rate of the first hydrolytic process.[1c] On the other hand, treatment of **NAMI-A** with equivalent amounts of the reductants induced the rapid and quantitative reduction to ruthenium(II) species, whose nature was elucidated by ^{1}H NMR spectroscopy.[3e]

We have now investigated by UV-vis and ^{1}H NMR spectroscopy the effect of the addition of equivalent amounts of ascorbic acid to physiological solutions of the dianionic and neutral dimers.

Anionic species. The case of $Na_2[\{trans\text{-}RuCl_4(Me_2SO\text{-}S)\}_2(\mu\text{-pyz})]$ **1a** will be described in more detail; for the sake of comparison, the reduction process of the corresponding mononuclear species, $Na[trans\text{-}RuCl_4(Me_2SO\text{-}S)(pyz)]$ **2a**, will be treated first. According to ^{1}H NMR evidence, after reduction **2a** behaves similarly to reduced **NAMI-A**.[3e] At 25 °C the dianionic complex $[trans\text{-}RuCl_4(Me_2SO\text{-}S)(pyz)]^{2-}$ (**2aA**, δ Me_2SO-*S* 3.65 (s); δ pyz 9.66 (m, $H^{2,6}$) and 8.70 (m, $H^{3,5}$)), derived by outer sphere electron transfer to **2a**, released a chloride rather rapidly (*ca.* 10 min) and was thus replaced by the monoaqua species $mer\text{-}[RuCl_3(Me_2SO\text{-}S)(pyz)(H_2O)]^-$ (**2aB**, δ Me_2SO-*S* 3.64 (s); δ pyz 9.52 (m, $H^{2,6}$) and 8.79 (m, $H^{3,5}$)).¶ Hydrolysis of a further chloride occurred at a slower rate, and only after *ca.* 15 min the resonances of a new monomeric species $[RuCl_2(Me_2SO\text{-}S)(pyz)(H_2O)_2]$ (**2aC**, δ Me_2SO-*S* 3.62 (s); δ pyz 9.45 (m, $H^{2,6}$) and 8.87 (m,$H^{3,5}$)) began to grow at the expense of **2aB**, which remained the prevailing species in solution up to 2 h, anyway. We have been unable to assign the geometry of **2aC**, since both the *cis* and *trans* isomers have enantiotopic Me_2SO-*S* methyl groups. Literature data about the *trans*-labilizing effect of chloride compared to oxygen available for pure aqua-chloride ruthenium-(III) and -(II) species do not seem to apply to complexes bearing other ligands. In fact, even though in ruthenium-(III) aqua-halide complexes chloride has a larger *trans*-influencing effect compared to oxygen,[22] stepwise chloride hydrolysis from **ICR** led to a mixture of roughly equal amounts of *cis* and *trans* diaqua species.[23] A similar inconsistency with literature data is observed in our case: while the rates of aquation of *cis*- and *trans*-$[RuCl_2(H_2O)_4]$ were calculated to be almost identical,[24] we found that, unless the resonances of the two geometrical isomers of **2aC** overlap, chloride hydrolysis from **2aB** was rather selective.

Reduction of complex **2a** induced also a change in the electronic absorptions. While the visible region was characterized by the usual intense halide to metal charge transfer band at 400 nm, immediately after reduction it showed an almost equally intense band at 394 nm. By analogy with the spectrum of $[Ru(NH_3)_5(pyz)]^{2+}$, this absorption was attributed to a MLCT transition from Ru^{II} to co-ordinated pyrazine.[21] In the case of **NAMI-A** the spectrum of the reduced species showed only weak MLCT absorptions in the region between 350 and 400 nm, typical of ruthenium(II) chloride-dmso complexes with imidazole.[25]

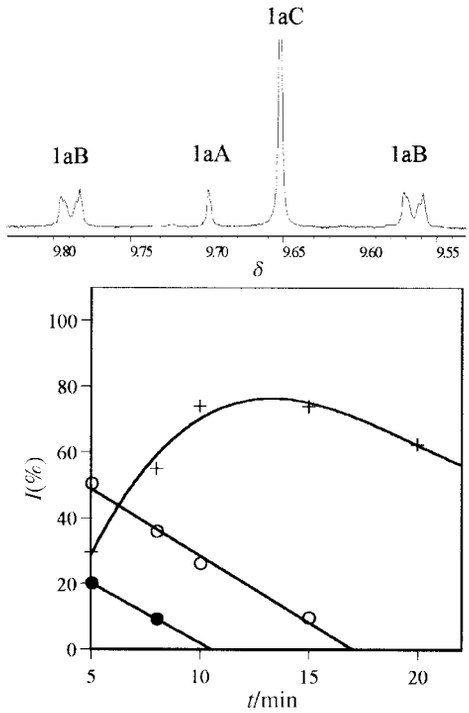

Fig. 7 Top: ^{1}H NMR spectrum (region of pyrazine resonances) of $Na_2[\{trans\text{-}RuCl_4(Me_2SO\text{-}S)\}_2(\mu\text{-pyz})]$ **1a** immediately after reduction with ascorbic acid (D_2O, phosphate buffer pH* 7.4, [Ru] = 12 mmol dm^{-3}). Bottom: concentration time profile of dimers **1aA** (●), **1aB** (○), and **1aC** (+) during the first 25 min after reduction of **1a** (25 °C).

As for the monomeric complex **2a**, the NMR spectrum of **1a** taken immediately after the addition of one equivalent of ascorbic acid showed sharp peaks exclusively, indicating that complete reduction of paramagnetic ruthenium(III) to diamagnetic ruthenium(II) species occurred. The region of bridging pyrazine resonances was characterized by two singlets and a pair of multiplets (Fig. 7), corresponding to three species whose relative abundance changed rather rapidly with time. The two species characterized by equivalent pyrazine protons must be symmetrical, while the other is obviously non-symmetrical. At 25 °C the singlet at δ 9.70 disappeared within less than 10 min and was therefore attributed to the tetraanionic symmetrical dimer $[\{trans\text{-}RuCl_4(Me_2SO\text{-}S)\}_2(\mu\text{-pyz})]^{4-}$ **1aA** derived by electron transfer to **1a**. Stepwise chloride hydrolysis from this led first to the non-symmetrical species $[\{trans\text{-}RuCl_4(Me_2SO\text{-}S)\}(\mu\text{-pyz})\{mer\text{-}RuCl_3(Me_2SO\text{-}S)(H_2O)\}]^{3-}$ **1aB** (δ H_{pyz} = 9.78 (m) and 9.56 (m)), which was in turn replaced within *ca.* 20 min by the symmetrical dianion $[\{mer\text{-}RuCl_3(Me_2SO\text{-}S)(H_2O)\}_2(\mu\text{-pyz})]^{2-}$ **1aC** (δ H_{pyz} = 9.65 (s)). The relative concentration of **1aC** reached a maximum within *ca.* 15 min and then decreased slowly toward a series of new species (see below). Each one of the reduced dimeric species **1aA**–**1aC** was also characterized by a singlet resonance for Me_2SO-*S* at about δ 3.68, partially overlapped with those of the two other species; the amount of free sulfoxide (crystallization molecules) did not increase appreciably with time. Integration of the pyrazine signals allowed us to draw the concentration time profile of the first three species formed after reduction of **1a** (Fig. 7).

Even though the diaqua dimer **1aC** is relatively inert, further stepwise aquation occurred leading to several new compounds;

¶ Very likely at pH* 7.4 partial or complete deprotonation of this and of the following aqua species to form hydroxo complexes occurs; see also ref. 23.

by far the most abundant was first a non-symmetrical species, presumably [{*mer*-$RuCl_3(Me_2SO$-*S*)(H_2O)}(μ-pyz){$RuCl_2(Me_2$-SO-*S*)$(H_2O)_2$}]$^-$ **1aD** (δ H_{pyz} 9.73 (m) and 9.58 (m); δ Me_2SO-*S* (tentatively) 3.64 (s)), from which another symmetrical dimer, [{$RuCl_2(Me_2SO$-*S*)$(H_2O)_2$}$_2$(μ-pyz)] **1aE** (δ H_{pyz} 9.66 (s); δ Me_2-SO-*S* (tentatively) 3.66 (s)), grew with time (Scheme 2). Approximately equal amounts of **1aC**, **1aD**, and **1aE** were

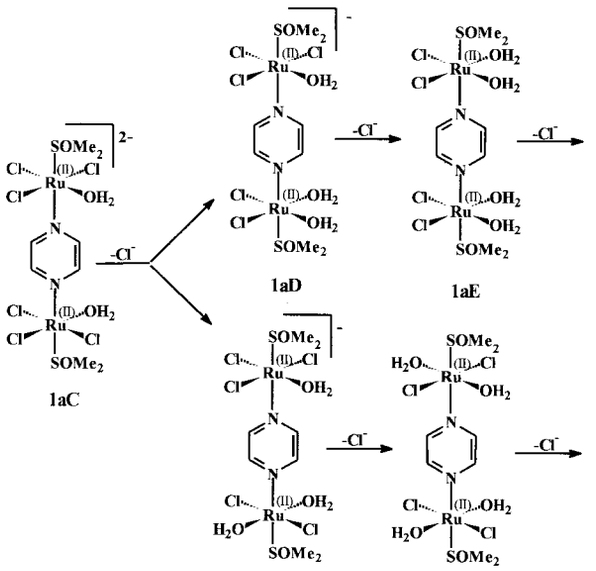

Scheme 2 Evolution of the main species (t > 1 h) obtained in physiological solution after reduction of Na_2[{*trans*-$RuCl_4(Me_2SO$-*S*)}$_2$(μ-pyz)] **1a** by addition of one equivalent of ascorbic acid (25 °C).

found after two hours at 25 °C. As for the monomeric species, we were unable to assign a *cis* or *trans* geometry to **1aD** and **1aE**; however, we notice that also in this case chloride hydrolysis from **1aC** occurred in a quite selective manner. Finally, beginning *ca.* 30 min after reduction, some very small signals attributable to mononuclear species **2aB** and **2aC** became detectable and increased very slowly with time.

Similarly, a careful examination of the time-driven ^{1}H NMR spectra of dimers **1b**–**1e** after reduction (same experimental conditions) allowed us to assign most of the resonances of the main species derived from stepwise aquation. The symmetrical or non-symmetrical nature of each species was established according to the number of resonances of the bridging ligand (δ $H^4 = \delta$ H^6 in symmetrically bridging pym; δ $H^{2,6} = \delta$ $H^{2',6'}$ and δ $H^{3,5} = \delta$ $H^{3',5'}$ in symmetrically bridging bipy, etbipy and prbipy). Overall, dimers **1b**–**1e** behave similarly to **1a** after reduction; a qualitative comparison of the hydrolytic rates showed that reduced **1b** has the fastest kinetics (the first two aquation steps were almost complete within 3 min), while reduced **1c**–**1e** are relatively more inert (the first two aquation steps were almost complete within 30 min and the corresponding dianionic dimers **1cC**–**1eC** prevailed in solution for up to 3 h). Even though the NMR data showed that the dimeric structure is generally robust also after reduction, formation of monomeric species bearing the terminal L ligand was appreciable for **1b** and **1d**. For **1c** and **1e** precipitates having the same color as that of the solution, presumably neutral aqua or hydroxo dimers, began to form *ca.* 1 h after reduction. In no case was air oxidation to ruthenium(III) species or formation of polyoxo species observed.

The reduction of the dimeric compounds was also accompanied by dramatic changes of the absorption bands in the visible region of the spectrum, which strongly depended on the nature of the bridging ligand (see Experimental section). For example, upon reduction of **1a** the solution turned from orange to dark red; correspondingly the 391 nm main absorption band was replaced by a more intense and broad band centered at 447

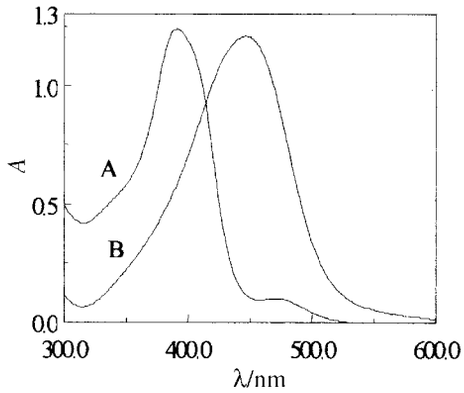

Fig. 8 Electronic absorption spectra of Na_2[{*trans*-$RuCl_4(Me_2$-SO-*S*)}$_2$(μ-pyz)] **1a** before (curve A) and immediately after reduction with ascorbic acid (curve B) (0.1 mol dm^{-3} phosphate buffer, pH 7.4, 0.9% NaCl).

nm (Fig. 8), attributable to a $t_{2g} \longrightarrow \pi^*$ charge-transfer absorption as in the case of [{$Ru(NH_3)_5$}$_2$(μ-pyz)]$^{4+}$.[10a] In all cases the stepwise aquation of the reduced species induced a slight hyperchromic shift and a decrease of the intensity for the main absorption band.

Neutral species. Even though the scarce solubility of the neutral dimer [{*mer*,*cis*-$RuCl_3(Me_2SO$-*S*)$(Me_2SO$-*O*)}$_2$(μ-pyz)] **3a** in physiological solution prevented the investigation of its behavior, we found that in the presence of equivalent amounts of ascorbic acid rapid reduction occurred which led to soluble species. Hence we undertook an NMR study of the reduction products of **3a**; as in the case of the dianionic dimers, for the sake of clarity the reduction process of the corresponding mononuclear species, *mer*,*cis*-[$RuCl_3(Me_2SO$-*S*)$(Me_2SO$-*O*)-(pyz)] **4a**, will be treated first.

The most relevant feature in the ^{1}H NMR spectrum of complex **4a** after reduction is the absence of signals for O-bonded dmso: the region of dmso resonances showed a peak for free sulfoxide (δ 2.72, accounting for 10% of total sulfoxide) and several singlets for Me_2SO-*S* ligands. This finding unambiguously indicated that *O* to *S* linkage isomerization of equatorial dmso, accompanied by its partial dissociation, occurred upon reduction of the ruthenium center, leading to *mer*,*cis*-[$RuCl_3(Me_2SO$-*S*$)_2$(pyz)]$^-$ **4aA** and *mer*-[$RuCl_3(Me_2$-SO-*S*)(H_2O)(pyz)]$^-$ **4aX**, respectively (Scheme 3). Linkage

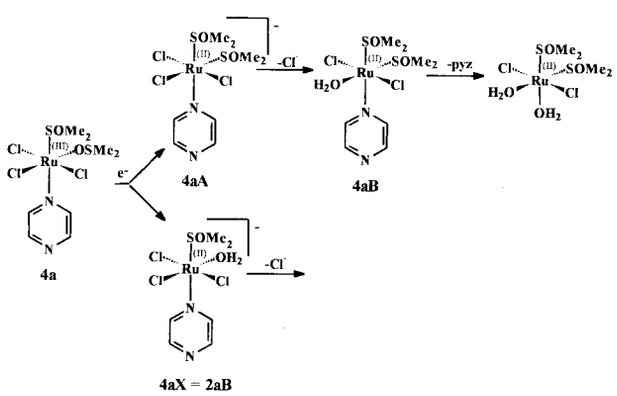

Scheme 3 Main species found in physiological solution after reduction of *mer*,*cis*-[$RuCl_3(Me_2SO$-*S*)$(Me_2SO$-*O*)(pyz)] **4a** by addition of one equivalent of ascorbic acid (25 °C).

isomerization of ruthenium-bound dmso induced by a change in the oxidation state of the metal is a well documented case.[26,27]

The resonances of complex **4aX** (δ Me_2SO-*S* 3.64 (s); δ pyz 9.52 (m, $H^{2,6}$) and 8.79 (m, $H^{3,5}$)) are coincident with those of **2aB**, thus unambiguously establishing the geometry of this

species. According to integration **4aX** represents *ca.* 20% of the total ruthenium(II) species. In accordance with the geometry of **4aA**, its spectrum has two equally intense singlets at δ 3.44 and 3.39 for the two inequivalent Me_2SO-*S* ligands, each bearing enantiotopic methyl groups (δ pyz 9.27 ($H^{2,6}$) and 8.61 ($H^{3,5}$)). The resonances of **4aA** were replaced within 30 min by the signals of a new species, **4aB** (δ Me_2SO-*S* 3.39 (s) and 3.33 (s); δ pyz 9.24 (m, $H^{2,6}$) and 8.70 (m, $H^{3,5}$)), derived from **4aA** upon chloride hydrolysis. The pattern of Me_2SO-*S* resonances of **4aB** is compatible only with a *trans* geometry for the two remaining chlorides; hence, in accordance with the larger *trans*-labilizing effect of Me_2SO-*S* compared to Cl, in **4aA** selective hydrolysis of the chloride *trans* to Me_2SO-*S* must occur. No experimental evidence was found for a *cis*,*cis*,*cis*-[$RuCl_2(Me_2SO$-*S*$)_2$(pyz)-(H_2O)] species, derived from **4aA** upon hydrolysis of one of the two *trans* chlorides and for which four equally intense Me_2SO-*S* methyl resonances, each accounting for a diastereotopic group, would be expected. Even though compound **4aB** is relatively inert and is the prevailing species in solution up to two hours, hydrolysis of pyrazine, rather than of further chlorides, slowly occurred. In the NMR spectrum this process was characterized by the contemporaneous growth of the resonances for free pyrazine at δ 8.64 and for co-ordinated dmso in *trans*,*cis*,*cis*-[$RuCl_2(Me_2SO$-*S*$)_2(H_2O)_2$] at δ 3.34;‖ for long observation times (>2 h) small amounts of the dimer [{*cis*,*cis*,*cis*-$RuCl_2(Me_2SO$-*S*$)_2(H_2O)\}_2$(μ-pyz)] (singlet for bridging pyz at δ 9.30, see below) formed.

The behavior of dimer **3a** after reduction with ascorbic acid recalled closely that of the corresponding monomer **4a**, but was further complicated because *O* to *S* linkage isomerization of equatorial dmso (which led to [{*mer*,*cis*-$RuCl_3(Me_2SO$-*S*$)_2\}_2$-(μ-pyz)]$^{2-}$ **3aA**, Scheme 4), was accompanied by partial

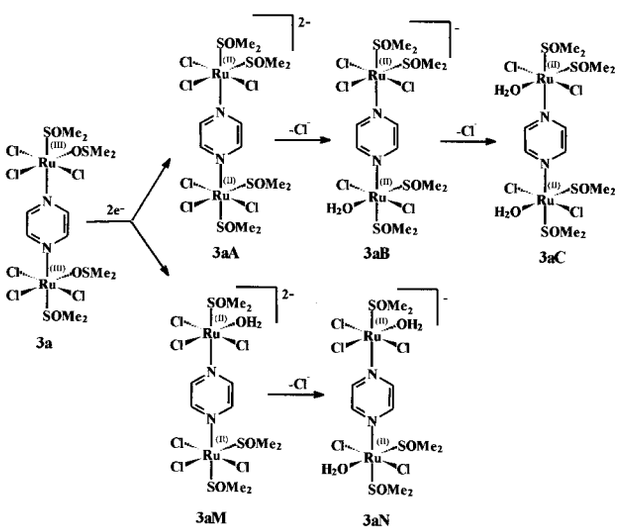

Scheme 4 Main species found in physiological solution after reduction of [{*mer*,*cis*-$RuCl_3(Me_2SO$-*S*$)(Me_2SO$-*O*$)\}_2$(μ-pyz)] **3a** by addition of one equivalent of ascorbic acid (25 °C).

hydrolysis of the ligand either from only one or from both ruthenium centers, yielding [{*mer*,*cis*-$RuCl_3(Me_2SO$-*S*$)_2\}$-(μ-pyz){*mer*,*cis*-$RuCl_3(Me_2SO$-*S*$)(H_2O)\}]^{2-}$ **3aM** (Scheme 4) and minor amounts of [{*mer*,*cis*-$RuCl_3(Me_2SO$-*S*$)(H_2O)\}_2$-(μ-pyz)]$^{2-}$ **3aX** (not reported in Scheme 4), respectively. According to integration of pyz resonances, the relative abundance of **3aA**, **3aM**, and **3aX** (including their hydrolytic products, see below) is 64, 33, and 3%, respectively. Despite the overlap of many peaks, in particular in the region of sulfoxide methyls, a careful examination of the spectral evolution allowed us to assign most of the resonances of the main species, according to the following general rules: (i) methyl groups of Me_2SO-*S* resonate between δ 3.6 and 3.7 when bound to *mer*-[$RuCl_3$-(Me_2SO-*S*)(H_2O)($\frac{1}{2}$pyz)]$^-$ units, and between δ 3.3 and 3.5 when bound to *mer*,*cis*-[$RuCl_3(Me_2SO$-*S*$)_2(\frac{1}{2}$pyz)]$^-$ units (see above for reduced **4a**); (ii) bridging pyrazine gives a singlet when the two linked ruthenium(II) units are equal, and two multiplets when they are different.

The resonances of the symmetrical dimer **3aA** (δ Me_2SO-*S* 3.45 (s) and 3.40 (s); δ pyz 9.24 (s)) decreased rapidly and within 10 min were replaced by those of the monoanion **3aB** (δ Me_2-SO-*S* (tentatively) 3.45 (s), 3.39 (s), 3.34 (s), and 3.31 (s); δ pyz 9.32 (m) and 9.24 (m)) and of the neutral symmetrical species **3aC** (δ Me_2SO-*S* 3.40 (s) and 3.35 (s); δ pyz 9.30 (s)), derived by stepwise selective hydrolysis of the chlorides *trans* to the Me_2SO-*S* ligands (Scheme 4). Species **3aB** disappeared almost completely within 1 h, while **3aC** is relatively inert and maintained a relevant concentration for observation times up to 3 h.

As for **3aA**, the monoaqua dianionic species **3aM** (δ Me_2SO-*S* (tentatively) 3.65 (s), 3.38 (s), and 3.37 (s); δ pyz 9.48 (m) and 9.39 (m)) hydrolyzed the chloride *trans* to Me_2SO-*S* rather rapidly and within 10 min its resonances were replaced by those of the monoanion **3aN** (Scheme 4, δ Me_2SO-*S* 3.65 (s), 3.43 (s), and 3.36 (s); δ pyz 9.57 (m) and 9.39 (m)), which is rather inert and, together with **3aC**, was the main species in solution in the first hour after reduction.

The resonances of the diaqua neutral dimer **3aX** (δ Me_2SO-*S* 3.68 (s); δ pyz 9.65 (s)) are equal to those of **1aC**, unambiguously establishing its geometry.

Partial dissociation of the dimeric structure also occurred and the resonances of complex **4aB** slowly, but steadily, grew with time; **4aB** represented *ca.* 25% of the species in solution after 3 h.

Conclusion

We reported here the synthesis and characterization of symmetrical dianionic and neutral ruthenium(III) dimers belonging to two new classes of formula Na_2[{*trans*-$RuCl_4(Me_2SO$-*S*$)\}_2$-(μ-L)] **1** and [{*mer*,*cis*-$RuCl_3(Me_2SO$-*S*$)(Me_2SO$-*O*$)\}_2$(μ-L)] **3**, respectively, with L = a ditopic aromatic N-ligand. The synthetic procedures used exploited the known reactivity of the ruthenium sulfoxide precursors toward N-ligands. Each ruthenium center in **1** and **3** has a co-ordination environment similar to that of known anionic and neutral monomeric ruthenium(III) complexes endowed with a specific antimetastatic activity against animal model tumors. The new dimeric species are being investigated to this regard.[8,19]

The dianionic dimers **1a**–**1e** are quite soluble in aqueous solution and their chemical behavior under physiological conditions was thoroughly investigated. We showed that, at 25 °C and pH 7.4, the dimeric structure is maintained and, similarly to the mononuclear analogs, in a first step they undergo rather slow hydrolysis of one chloride ligand from each $RuCl_4$ unit to yield the relatively inert diaqua species [{*mer*-$RuCl_3(Me_2SO$-*S*$)$-(H_2O)$\}_2$(μ-L)]. The dimers with bridging pyrazine and pyrimidine (**1a**, **1b**) were markedly more inert than the others. At physiological pH dimers **1a**–**1e** are also easily and quantitatively reduced by equivalent amounts of ascorbic acid to the corresponding $Ru^{II/II}$ dimers which, in turn, undergo stepwise aquation. Since the reduction processes might occur also *in vivo*, investigation of the chemical behavior of the $Ru^{II/II}$ dimers is relevant to understanding the biological mechanism of action of these compounds and was thus investigated in detail. In the reduced dimers the opposite order of hydrolytic rates was found compared to the $Ru^{III/III}$ dimers, *i.e.* reduced **1a** and **1b** aquated faster than reduced **1c**–**1e**. Interestingly, even though the rates of hydrolysis for ruthenium(II) chloride complexes are usually much more rapid than those for the corresponding ruthenium(III) chlorides,[24] we found that the rates of aquation

‖ The same species is obtained upon dissolution of *trans*-[$RuCl_2$-(Me_2SO-*S*)$_4$] in aqueous solution; see also ref. 28.

of $Ru^{III/III}$ dimers are roughly comparable to those of the corresponding $Ru^{II/II}$ species with the same net charge; moreover, chloride hydrolysis from the reduced monoaqua species was rather selective, yielding one main diaqua species. Overall, these findings indicate that the presence of Me_2SO-*S* and L in the co-ordination sphere of ruthenium has a large influence on the aquation rates compared to pure aqua-chloride compounds.

The neutral dimer **3a** is scarcely soluble in aqueous solution, but gives soluble dimeric species upon reduction with ascorbic acid. We proved that reduction is accompanied by *O* to *S* linkage isomerization and by partial dissociation of the equatorial dmso.

Although the mechanism of action of the antimetastatic *trans*-$[RuCl_4(Me_2SO\text{-}S)(L)]^-$ complexes is not understood yet, it has nevertheless been proved that these compounds, after hydrolysis of at least one chloride, may interact *in vitro* with DNA[29] and with proteins such as transferrin[30] and albumin.[31] We have proved that the dimeric structure of the new compounds is quite robust, both in the $Ru^{III/III}$ and in the $Ru^{II/II}$ form, and that they undergo hydrolytic reactions similar to those of the monomeric analogs. However, while the monomeric species, like **NAMI-A**, are either mono- or bi-functional binders after chloride hydrolysis, the new dimers might behave as bi- or even tetra-functional binders. Thus, it is likely that the co-ordination of the dimers to biological targets might lead to adducts which are different from those of the mononuclear species. For example, co-ordination to the histidine residues on proteins and/or to nucleobases of DNA might lead to crosslinking reactions.

Finally, although the new ruthenium(III) dimeric species described here were developed with the specific aim of assessing their antineoplastic properties, they nevertheless represent new entries in the general Creutz–Taube family of ruthenium dimers. In particular, to our knowledge they are the first examples of structurally characterized anionic and neutral ruthenium(III) dimers and, by virtue of their facile reduction, they might represent a valuable starting point for the synthesis of mixed-valent dinuclear species. Indeed, there is continued interest in understanding the electronic structures of symmetrical mixed-valent dinuclear complexes; compared to the classical Creutz–Taube dimers, the compounds described here might allow one to explore the effect of replacement of the exclusively σ-donating amines by negatively charged (Cl^-) and π-acceptor (Me_2SO-*S*) ligands which might compete with the bridging ligand for π back donation from the metal.

Experimental

Materials

The bridging ligands were purchased from Aldrich, except prbipy from Lancaster, and used as received. Electronic absorption spectra were recorded in quartz cells with a JASCO UV/vis V500 spectrophotometer equipped with a Peltier thermostatic unit. Physiological solution: 0.1 mol dm^{-3} phosphate buffer, pH 7.4, 0.9% NaCl. Infrared spectra were obtained on a Perkin-Elmer 983 G spectrometer. Nujol mulls were recorded between CsI windows. The ^1H NMR spectra were collected at 400 MHz on a JEOL EX 400 FT spectrometer. Deuteriated solvents were purchased from Aldrich. All spectra were recorded at room temperature with 4,4-dimethyl-4-silapentane-1-sulfonate (DSS) as an internal standard for D_2O solutions and residual non-deuteriated solvent signal as reference for dmso-d_6 and $CDCl_3$ spectra. An inversion recovery pulse sequence (π–t_1–$\pi/2$) was applied for recording the spectra of the paramagnetic compounds (spectral window 30.000 Hz, pulse delay 0.5 s); with $t_1 = 100$ ms the resonances of molecules not co-ordinated to Ru^{III} were negative, while those of the co-ordinated ligands were positive. A 0.1 mol dm^{-3} pH* 7.4 phosphate–D_2O buffer (pH meter reading from D_2O solutions) containing 0.9% NaCl was used for NMR experiments involving reduction of the dimers; complex concentration was 6 mmol dm^{-3}.

Preparation of the complexes

The complexes Na[*trans*-$RuCl_4(Me_2SO\text{-}S)_2$] and *mer*-$[RuCl_3(Me_2SO)_3]$ were synthesized according to literature procedures.[27]

Na_2[{*trans*-$RuCl_4(Me_2SO\text{-}S)$}$_2$(μ-pyz)] 1a. A 0.200 g amount of Na[*trans*-$RuCl_4(Me_2SO\text{-}S)_2$] (0.48 mmol) was dissolved in 2 mL of dmso, then 0.019 g of pyrazine (0.24 mmol) dissolved in 5 mL of acetone was added with magnetic stirring. The orange solution was filtered over a fine paper filter. Red-orange microcrystals of the product formed from the clear solution after some hours at room temperature and were collected by filtration, washed with cold acetone and diethyl ether, and vacuum dried at r.t. (0.20 g, 82%). The complex contains three dmso molecules and one H_2O molecule of crystallization and is better formulated as $Na_2[\{trans\text{-}RuCl_4(Me_2SO\text{-}S)\}_2(\mu\text{-pyz})]\cdot 3Me_2SO\cdot 1H_2O$ (Found: C, 16.6; H, 3.52; N, 2.71. $C_{14}H_{36}Cl_8N_2Na_2O_6Ru_2S_5$ requires C, 16.5, H, 3.55; N, 2.74%); λ_{max}/nm (water) 470 (ε/dm^3 mol^{-1} cm^{-1} 1000) and 390 (10900); (immediately after reduction) 447 (10100); $\tilde{\nu}_{max}$/cm^{-1} 1074vs (Me_2SO-*S*), 437m (Ru–S), and 330s (Ru–Cl) (Nujol); δ_H (D_2O) −14.3 (br, Me_2SO-*S*).

Na_2[{*trans*-$RuCl_4(Me_2SO\text{-}S)$}$_2$(μ-pym)] 1b. A procedure similar to that described above for complex **1a** was followed (yield 66%). The complex contains three dmso molecules and one H_2O molecule of crystallization and can be better formulated as $Na_2[\{trans\text{-}RuCl_4(Me_2SO\text{-}S)\}_2(\mu\text{-pym})]\cdot 3Me_2SO\cdot H_2O$ (Found: C, 16.6; H, 3.49; N, 2.69. $C_{14}H_{36}Cl_8N_2Na_2O_6Ru_2S_5$ requires C, 16.5, H, 3.55; N, 2.74); λ_{max}/nm (water) 470 (ε/dm^3 mol^{-1} cm^{-1} 900) and 401 (7400); (immediately after reduction) 354 (5600); $\tilde{\nu}_{max}$/cm^{-1} 1081vs (Me_2SO-*S*), 433m (Ru–S), and 341s (Ru–Cl) (Nujol); δ_H (D_2O) −14.4 (br, Me_2SO-*S*), −9.8 (br, pym), −9 (vbr, pym), and 11.4 (br, pym).

Na_2[{*trans*-$RuCl_4(Me_2SO\text{-}S)$}$_2$(μ-bipy)] 1c. A procedure similar to that described above for complex **1a** was followed (yield 69%). As an average, the complex contains three dmso molecules and one H_2O molecule of crystallization and can be better formulated as $Na_2[\{trans\text{-}RuCl_4(Me_2SO\text{-}S)\}_2(\mu\text{-bipy})]\cdot 3Me_2SO\cdot H_2O$ (Found: C, 21.4; H, 3.79; N, 2.25. $C_{20}H_{40}Cl_8N_2Na_2O_6Ru_2S_5$ requires C, 21.9; H, 3.68; N, 2.55%)** λ_{max}/nm (water) 462 (ε/dm^3 mol^{-1} cm^{-1} 970) and 393 (7400); (immediately after reduction) 384 (11000); $\tilde{\nu}_{max}$/cm^{-1} 1096vs (Me_2SO-*S*), 434m (Ru–S), and 338s (Ru–Cl) (Nujol); δ_H (D_2O) −14.4 (br, Me_2SO-*S*), −10 (vbr, $H^{2,6+2',6'}$ bipy), and −4.4 (br, $H^{3,5+3',5'}$ bipy).

Na_2[{*trans*-$RuCl_4(Me_2SO\text{-}S)$}$_2$(μ-etbipy)] 1d. A procedure similar to that described above for complex **1a** was followed (yield 66%). As an average, the complex contains three dmso molecules and one H_2O molecule of crystallization and can be better formulated as $Na_2[\{trans\text{-}RuCl_4(Me_2SO\text{-}S)\}_2(\mu\text{-etbipy})]\cdot 3Me_2SO\cdot H_2O$ (Found: C, 22.2; H, 3.78; N, 2.46. $C_{22}H_{44}Cl_8N_2Na_2O_6Ru_2S_5$ requires C, 23.5; H, 3.94; N, 2.49%);‖ λ_{max}/nm (water) 458 (ε/dm^3 mol^{-1} cm^{-1} 880) and 395 (6200); (immediately after reduction) 312 (10500); $\tilde{\nu}_{max}$/cm^{-1} 1050vs (Me_2SO-*S*), 436m (Ru–S), and 336s (Ru–Cl) (Nujol); δ_H (D_2O) −14.4 (br, Me_2SO-*S*), −11 (vbr, $H^{2,6+2',6'}$ etbipy), −4.4 (br, $H^{3,5+3',5'}$ etbipy), and −3.8 (br, $(CH_2)_2$).

Na_2[{*trans*-$RuCl_4(Me_2SO\text{-}S)$}$_2$(μ-prbipy)] 1e. This dimer was best prepared from pure acetone rather than from acetone–dmso mixtures like **1a**–**1d** (yield 80%). The complex was

** Water and, sometimes, acetone molecules can partially replace the dmso molecules of crystallization, thereby affecting the goodness and the reproducibility of elemental analysis.

Table 5 Crystal data and structure refinement for $Na_2[\{trans\text{-}RuCl_4(Me_2SO\text{-}S)\}_2(\mu\text{-pyz})]$ **1a**, $Na_2[\{trans\text{-}RuCl_4(Me_2SO\text{-}S)\}_2(\mu\text{-pym})]$ **1b**, $Na_2[\{trans\text{-}RuCl_4(Me_2SO\text{-}S)\}_2(\mu\text{-bipy})]$ **1c**, and $[\{mer,cis\text{-}RuCl_3(Me_2SO\text{-}S)(Me_2SO\text{-}O)\}_2(\mu\text{-pyz})]$ **3a**

	1a·3Me_2SO·H_2O	**1b**·3Me_2SO·H_2O	**1c**·5.6H_2O	**3a**·2$CHCl_3$
Formula	$C_{14}H_{36}Cl_8N_2Na_2O_6Ru_2S_5$	$C_{14}H_{36}Cl_8N_2Na_2O_6Ru_2S_5$	$C_{14}H_{31.2}Cl_8N_2Na_2O_{7.6}Ru_2S_2$	$C_{14}H_{30}Cl_{12}N_2O_4Ru_2S_4$
M	1020.47	1020.47	945.05	1046.18
T/K	298(2)	298(2)	298(2)	298(2)
Crystal system	Triclinic	Monoclinic	Monoclinic	Monoclinic
Space group	$P\bar{1}$	$P2_1/c$	$C2/c$	$P2_1/n$
a/Å	7.419(3)	11.371(1)	30.363(3)	10.770(3)
b/Å	11.048(2)	14.613(1)	7.561(1)	14.526(3)
c/Å	11.210(4)	22.578(1)	16.162(6)	11.764(3)
α/°	93.33(3)			
β/°	101.51(3)	96.415(8)	119.00(2)	100.07(1)
γ/°	92.61(3)			
U/Å^3	897.3(7)	3728.2(5)	3245(2)	1812.1(8)
Z	1	4	4	2
μ/mm^{-1}	1.78	1.72	1.78	1.97
Independent reflections	3502	6306	3900	5267
Reflections with $I > 2\sigma(I)$	1370	4457	2802	4043
Goodness of fit	1.07	1.03	1.01	1.03
$R[I > 2\sigma(I)]$	0.11	0.038	0.044	0.036
$wR2$	0.28	0.098	0.11	0.088

recrystallized from methanol upon addition of *n*-hexane (yield 55%); it contains, as an average, three H_2O molecules of crystallization and can be better formulated as $Na_2[\{trans\text{-}RuCl_4(Me_2SO\text{-}S)\}_2(\mu\text{-prbipy})]\cdot 3H_2O$ (Found: C, 21.8; H, 3.24; N, 2.98. $C_{17}H_{32}Cl_8N_2Na_2O_5Ru_2S_2$ requires C, 21.7; H, 3.40; N, 2.98%); λ_{max}/nm (water) 458 (ε/dm^3 mol^{-1} cm^{-1} 700) and 395 (5000); (immediately after reduction) 310 (10300); $\tilde{\nu}_{max}$/cm^{-1} 1086vs (Me_2SO-*S*), 430m (Ru–S), and 330s (Ru–Cl) (Nujol); δ_H (D_2O) −14.4 (br, Me_2SO-*S*), −11 (vbr, $H^{2,6+2',6'}$ prbipy), −4.4 (br, $H^{3,5+3',5'}$ prbipy), and −3.8 (br, $(CH_2)_3$).

Na[*trans*-RuCl$_4$(Me$_2$SO-*S*)(pyz)] 2a. A 0.200 g amount of $Na[trans\text{-}RuCl_4(Me_2SO\text{-}S)_2]$ (0.48 mmol) was dissolved in 2 mL of dmso, then 0.190 g of pyrazine (2.4 mmol) dissolved in 5 mL of acetone was added with magnetic stirring. The orange solution was filtered over a fine paper filter. Red-orange microcrystals of the product formed from the clear solution after some hours at room temperature and were collected by filtration, washed with cold acetone and diethyl ether, and vacuum dried at r.t. (168 mg, 60%). The complex contains dimethyl sulfoxide and water molecules of crystallization and can be better formulated as $Na[trans\text{-}RuCl_4(Me_2SO\text{-}S)(pyz)]\cdot 1.5Me_2SO\cdot 0.5H_2O$ (Found: C, 19.6; H, 3.42; N, 5.0. $C_9H_{20}Cl_4N_2NaO_3RuS_{2.5}$ requires C, 19.6, H, 3.66; N, 5.1%);** λ_{max}/nm (water) 470 (ε/dm^3 mol^{-1} cm^{-1} 500) and 400 (4400); (immediately after reduction) 394 (4500); $\tilde{\nu}_{max}$/cm^{-1} 1590m (pyz), 1104vs (Me_2SO-*S*), 429m (Ru–S), 346, and 332s (Ru–Cl) (Nujol); δ_H (D_2O) −13.9 (br, Me_2SO-*S*), −7 (vbr, $H^{2,6}$ pyz), and −2.2 (br, $H^{3,5}$ pyz).

[{*mer*,*cis*-RuCl$_3$(Me$_2$SO-*S*)(Me$_2$SO-*O*)}$_2$(μ-pyz)] 3a. A 0.100 g amount of *mer*-$[RuCl_3(Me_2SO)_3]$ (0.23 mmol) was dissolved in 5 mL of $CHCl_3$ and 0.009 g of pyrazine (0.112 mmol) was added. In a few minutes at r.t. the solution turned cloudy and was maintained with magnetic stirring at room temperature overnight. The product was then collected by filtration, washed with cold $CHCl_3$ and diethyl ether and vacuum dried at r.t. (63 mg, 70%). The complex contains one $CHCl_3$ molecule of crystallization and can be better formulated as $[\{mer,cis\text{-}RuCl_3(Me_2SO\text{-}S)(Me_2SO\text{-}O)\}_2(\mu\text{-pyz})]\cdot CHCl_3$ (Found: C, 16.8; H, 3.08; N, 3.07. $C_{13}H_{29}Cl_9N_2O_4Ru_2S_4$ requires C, 16.8; H, 3.15; N, 3.02%); λ_{max}/nm (dmso) 378 (ε/dm^3 mol^{-1} cm^{-1} 11000); $\tilde{\nu}_{max}$/cm^{-1} 1106vs (Me_2SO-*S*), 893vs (Me_2SO-*O*), 494m (Ru–O), 426m (Ru–S), and 341s (Ru–Cl) (Nujol); δ_H (dmso-d_6) −13.2 (br, Me_2SO-*S*) and 8.3 (br, Me_2SO-*O*).

***mer*,*cis*-[RuCl$_3$(Me$_2$SO-*S*)(Me$_2$SO-*O*)(pyz)] 4a.** A 0.100 g amount of *mer*-$[RuCl_3(Me_2SO)_3]$ (0.23 mmol) was dissolved in 7 mL of $CHCl_3$ and 0.055 g of pyrazine (0.69 mmol) was added. In a few minutes at room temperature the solution turned cloudy and was filtered over a fine paper filter. After overnight standing at room temperature, the clear solution turned from orange-red to brown-yellow. The solution was then vacuum evaporated to 2 mL and a few drops of diethyl ether were added. Brown-yellow crystals of the product separated from the solution after some hours at 4 °C and were collected by filtration, washed with cold $CHCl_3$ and diethyl ether and vacuum dried at r.t. (71 mg, 70%) (Found: C, 22.1; H, 3.56; N, 6.26. $C_8H_{16}Cl_3N_2O_2RuS_2$ requires C, 21.6, H, 3.63; N, 6.31%); λ_{max}/nm (dmso) 432 (sh) (ε/dm^3 mol^{-1} cm^{-1} 1200) and 372 (3300); $\tilde{\nu}_{max}$/cm^{-1} 1588m (pyz), 1098vs (Me_2SO-*S*), 912vs (Me_2SO-*O*), 488m (Ru–O), 422m (Ru–S), 353, and 337s (Ru–Cl) (Nujol); δ_H (dmso-d_6) −12.7 (br, Me_2SO-*S*), −5 (vbr, $H^{2,6}$ pyz), −0.6 (br, $H^{3,5}$ pyz), and 9.1 (br, Me_2SO-*O*).

X-Ray crystallographic studies

Crystals of complexes **1a**, **1b**, and **1c** were obtained by addition of polyethylene glycol (PEG) to saturated aqueous solutions of the anionic dimers. Those of **3a** grew from the mother-liquor of the synthetic reaction after filtration of the first batch of precipitate.

Diffraction data were obtained using the ω–2θ scan technique on a CAD4 Enraf-Nonius single-crystal diffractometer equipped with a graphite monochromator and Mo-Kα radiation ($\lambda = 0.7107$ Å). Three standard reflections, measured at regular intervals throughout the data collections, showed no noticeable variation in intensity for all crystals. The data were corrected for Lorentz-polarization effects and absorption (empirical ψ scan method). All the structures were solved by conventional Patterson [32] and Fourier analyses, and refined on F^2 by the full-matrix anisotropic least-squares method using the SHELXL 93 program.[33]

Three disordered molecules of dmso and one of water were located on the ΔF maps of complexes **1a** and **1b**, while for **1c** 5.6 disordered water molecules for complex unit were found. For this complex also the sodium cation was found to be distributed over two positions. The ΔF map of **3a** revealed the presence of two disordered chloroform molecules for complex unit. The disorder was particularly severe for **1a**, in correspondence to the very poor quality of the crystals. The final cycles with the fixed contribution of hydrogen atoms, except those of the solvent

molecules, converged to the $R1$ and $wR2$ factors reported in Table 5.

CCDC reference number 186/1616.

See http://www.rsc.org/suppdata/dt/1999/3361/ for crystallographic files in .cif format.

Acknowledgements

This work was supported by Ministero dell'Università e della Ricerca Scientifica e Tecnologica in the frame of the Project "Pharmacological and Diagnostic Properties of Metal Complexes" (co-ordinator Professor G. Natile), by Polytech s.r.l. (Science Park of Trieste), and by EU COST Action D8 (Project D8/96/0017). We thank Johnson Matthey for a generous loan of hydrated $RuCl_3$.

References

1 (*a*) G. Mestroni, E. Alessio, G. Sava, S. Pacor and M. Coluccia, in *Metal Complexes in Cancer Chemotherapy*, ed. B. K. Keppler, VCH, Weinheim, 1993, pp. 157–185; (*b*) G. Sava, S. Pacor, E. Alessio, G. Mestroni, R. Gagliardi, M. Cocchietto and M. Coluccia, *Drugs of the Future*, 1993, **18**, 894; (*c*) G. Mestroni, E. Alessio, G. Sava, S. Pacor, M. Coluccia and A. Boccarelli, *Metal-Based Drugs*, 1994, **1**, 41.

2 G. Mestroni, E. Alessio and G. Sava, *Int. Pat.*, WO 98/00431, 1998.

3 (*a*) G. Sava, I. Capozzi, K. Clerici, G. Gagliardi, E. Alessio and G. Mestroni, *Clin. Exp. Metastasis*, 1998, **16**, 371; (*b*) G. Sava, R. Gagliardi, M. Cocchietto, K. Clerici, I. Capozzi, M. Marella, E. Alessio, G. Mestroni and R. Milanino, *Pathol. Oncol. Res.*, 1998, **4**, 30; (*c*) G. Sava, K. Clerici, I. Capozzi, M. Cocchietto, R. Gagliardi, E. Alessio, G. Mestroni and A. Perbellini, *Anti-Cancer Drugs*, 1999, **10**, 129; (*d*) A. Bergamo, R. Gagliardi, V. Scarcia, A. Furlani, E. Alessio, G. Mestroni and G. Sava, *J. Pharmacol. Exp. Ther.*, 1999, **298**, 559; (*e*) G. Sava, E. Alessio, A. Bergamo and G. Mestroni, in *Topics in Biological Inorganic Chemistry*, eds. M. J. Clarke and P. J. Sadler, Springer-Verlag, Berlin and Heidelberg, 1999, vol. 1, pp. 143–169.

4 E. Alessio, G. Balducci, A. Lutman, G. Mestroni, M. Calligaris and W. M. Attia, *Inorg. Chim. Acta*, 1993, **203**, 205.

5 B. K. Keppler, W. Rupp, U. M. Juhl, H. Enders, R. Niebl and W. Balzer, *Inorg. Chem.*, 1987, **26**, 4366.

6 B. K. Keppler, M. Henn, U. M. Juhl, M. R. Berger, R. Niebl and F. E. Wagner, in *Ruthenium and Other Non-Platinum Metal Complexes in Cancer Chemotherapy*, ed. M. J. Clarke, Springer, Heidelberg, 1989, vol. 14, pp. 41–70.

7 N. Farrell, Y. Qu, U. Bierbach, M. Valsecchi and E. Menta, in *Cisplatin—Chemistry and Biochemistry of a Leading Anticancer Drug*, ed. B. Lippert, VHCA (Zurich) and Wiley-VCH (Weinheim), 1999, pp. 479–496; N. Farrell, *Comments Inorg. Chem.*, 1995, **16**, 373; Y. Qu, S. G. da Almeida and N. Farrell, *Inorg. Chim. Acta*, 1992, **201**, 123.

8 E. Alessio, E. Iengo, G. Mestroni and G. Sava, *It. Pat.*, MI99A000811, 1999.

9 M. D. Ward, *Chem. Soc. Rev.*, 1995, 121; B. J. Coe, T. J. Meyer and P. S. White, *Inorg. Chem.*, 1995, **34**, 593.

10 (*a*) C. Creutz and H. Taube, *J. Am. Chem. Soc.*, 1969, **91**, 3988; (*b*) C. Creutz and H. Taube, *J. Am. Chem. Soc.*, 1973, **95**, 1086; (*c*) S. A. Adeyemi, E. C. Johnson, F. J. Miller and T. J. Meyer, *Inorg. Chem.*, 1973, **12**, 2371; (*d*) C. Creutz, *Prog. Inorg. Chem.*, 1983, **30**, 1; (*e*) D. E. Richardson and H. Taube, *Coord. Chem. Rev.*, 1984, **60**, 107.

11 V. Balzani, A. Juris, M. Venturi, S. Campagna and S. Serroni, *Chem. Rev.*, 1996, **96**, 759.

12 F. Felix and A. Ludi, *Inorg. Chem.*, 1978, **17**, 1782.

13 F. M. Hornung, F. Baumann, W. Kaim, J. A. Olabe, L. D. Slep and J. Fiedler, *Inorg. Chem.*, 1998, **37**, 311.

14 Y. Chen and R. E. Shepherd, *Inorg. Chem.*, 1998, **37**, 1249.

15 J. P. Collman, J. T. McDevitt, C. R. Leinder, G. T. Yee, J. B. Torrance and W. A. Little, *J. Am. Chem. Soc.*, 1987, **109**, 4606.

16 C. K. Johnson, ORTEP II, Report ORNL-5138, Oak Ridge National Laboratory, Oak Ridge, TN, 1976.

17 M. Calligaris and O. Carugo, *Coord. Chem. Rev.*, 1996, **153**, 83.

18 S. Geremia, E. Alessio and F. Todone, *Inorg. Chim. Acta*, 1996, **253**, 87.

19 E. Alessio, E. Iengo, S. Zorzet, A. Bergamo, M. Coluccia, A. Boccarelli and G. Sava, *J. Inorg. Biochem.*, in press.

20 C. M. Duff and G. A. Heat, *J. Chem. Soc.*, *Dalton Trans.*, 1991, 2401.

21 P. Ford, De F. P. Rudd, R. Gaunder and H. Taube, *J. Am. Chem. Soc.*, 1968, **90**, 1187.

22 *Comprehensive Coordination Chemistry*, eds. G. Wilkinson, R. D. Gillard and J. A. McCleverty, Pergamon, Oxford, 1987, vol. 4, ch. 45, pp. 442–446.

23 O. M. Ni Dhubhghaill, W. R. Hagen, B. K. Keppler, K.-G. Lipponer and P. J. Sadler, *J. Chem. Soc.*, *Dalton Trans.*, 1994, 3305.

24 P. E. Dumas and E. E. Mercer, *Inorg. Chem.*, 1972, **11**, 531.

25 M. Henn, E. Alessio, G. Mestroni, M. Calligaris and W. M. Attia, *Inorg. Chim. Acta*, 1991, **187**, 39.

26 A. Yeh, N. Scott and H. Taube, *Inorg. Chem.*, 1982, **21**, 2542; M. Sano and H. Taube, *J. Am. Chem. Soc.*, 1991, **113**, 2327; A. Tomita and M. Sano, *Inorg. Chem.*, 1994, **33**, 5825; M. Sano and H. Taube, *Inorg. Chem.*, 1994, **33**, 705.

27 E. Alessio, G. Balducci, M. Calligaris, G. Costa, W. M. Attia and G. Mestroni, *Inorg. Chem.*, 1991, **30**, 609.

28 E. Alessio, G. Mestroni, G. Nardin, W. M. Attia, M. Calligaris, G. Sava and S. Zorzet, *Inorg. Chem.*, 1988, **27**, 4099.

29 G. Sava, S. Pacor, M. Coluccia, M. Mariggio, M. Cocchietto, E. Alessio and G. Mestroni, *Drug Invest.*, 1994, **8**, 150.

30 L. Messori, F. Kratz and E. Alessio, *Metal-Based Drugs*, 1996, **3**, 1.

31 L. Messori, P. Orioli, D. Vullo, E. Alessio and E. Iengo, unpublished work.

32 G. M. Sheldrick, *Acta Crystallogr.*, *Sect. A*, 1990, **46**, 467.

33 G. M. Sheldrick, SHELXL 93, Program for crystal structure refinement, Universität Göttingen, 1993.

Paper 9/04264D